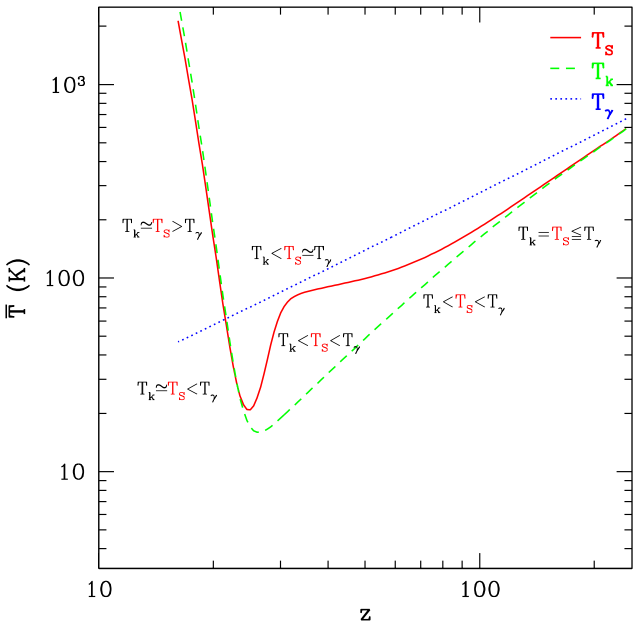

Figure 10. Evolution of the mean temperatures from 21cmFAST in our fiducial model. Solid, dashed and dotted curves show $T_{\rm S}$, $T_{\rm K}$ and T_γ, respectively.

(i) **Collisional coupling;** $\bar{T}_{\rm K} = \bar{T}_{\rm S} \leq T_\gamma$: At high redshifts, the IGM is dense, so the spin temperature is collisionally coupled to the gas kinetic temperature. The gas temperature is originally coupled to the CMB, but after decoupling cools adiabatically as $\propto (1+z)^{-2}$, faster than the CMB. The 21-cm brightness temperature offset from the CMB in this regime starts at zero, when all three temperatures are equal, and then becomes increasingly negative as $T_{\rm S}$ and $T_{\rm K}$ diverge more and more from T_γ. The fluctuations in δT_b are driven by the density field, as collisional coupling is efficient everywhere. In our fiducial model, this epoch corresponds to $100 \lesssim z$.

(ii) **Collisional decoupling;** $\bar{T}_{\rm K} < \bar{T}_{\rm S} < T_\gamma$: The IGM becomes less dense as the Universe expands. The spin temperature starts to decouple from the kinetic temperature, and begins to approach the CMB temperature again, thus δT_b starts rising towards zero. Decoupling from $T_{\rm K}$ occurs as a function of the local gas density, with underdense regions decoupling first. The power spectrum initially steepens, as small-scale density fluctuations drive the additional fluctuations of the collisional coupling coefficient. As the spin temperature in even the overdense regions finally decouples from the kinetic temperature, the power spectrum flattens again, and the mean signal drops as $\bar{T}_{\rm S} \rightarrow 0$. In our fiducial model, this epoch corresponds to $35 \lesssim z \lesssim 100$.

(iii) **Collisional decoupling → WF coupling transition;** $\bar{T}_{\rm K} < \bar{T}_{\rm S} \approx T_\gamma$: As the spin temperature throughout the IGM decouples from the kinetic temperature, the mean signal is faint and might disappear, if the first sources wait long enough to ignite. In our fiducial model, this transition regime doesn't really exist. In fact our first sources turn on before the spin temperature fully decouples from the kinetic temperature.

(iv) **WF coupling;** $\bar{T}_{\rm K} < \bar{T}_{\rm S} < T_\gamma$: The first astrophysical sources turn on, and begin coupling the spin temperature of the nearby IGM to the kinetic temperature through the WF effect (Lyα coupling). As the requirements for Lyα coupling are more modest than those to heat the gas through X-ray heating, the kinetic temperature keeps decreasing in this epoch. The mean brightness temperature offset from the CMB starts becoming more negative[25] again and can even reach values of $\delta T_b < -100$ mK. In our fiducial model, this epoch corresponds to $25 \lesssim z \lesssim 35$.

(v) **WF coupling → X-ray heating transition;** $\bar{T}_{\rm K} \sim \bar{T}_{\rm S} < T_\gamma$: Ly$\alpha$ coupling begins to saturate as most of the IGM has a spin temperature which is strongly coupled to the kinetic temperature. The mean spin temperature reaches a minimum value, and then begins increasing. A few underdense voids are left only weakly coupled as X-rays from the first sources begin heating the surrounding gas in earnest, raising its kinetic temperature. The 21-cm power spectrum steepens dramatically as small-scale overdensities now host hot gas, while on large scales the gas is uniformly cold as Lyα coupling saturates. As inhomogeneous X-ray heating continues, the large-scale power comes back up. In our fiducial model, this transition occurs around $z \sim 25$.

(vi) **X-ray heating;** $\bar{T}_{\rm K} = \bar{T}_{\rm S} < T_\gamma$: X-rays start permeating the IGM. The fluctuations in δT_b are now at their maximum, as regions close to X-ray sources are heated above the CMB temperature, $\delta T_b > 0$, while regions far away from sources are still very cold, $\delta T_b < 0$. A "shoulder" in the power spectrum, similar to that seen in the epoch of reionization (e.g. McQuinn et al. 2007), moves from small scales to large scales. X-rays eventually heat the entire IGM, and 21-cm can only be seen in emission. The power spectrum falls as this process nears completion. In our fiducial mode, this epoch corresponds to $18 \lesssim z \lesssim 25$.

(vii) **X-ray heating → reionization transition;** $\bar{T}_{\rm K} = \bar{T}_{\rm S} > T_\gamma$: X-rays have heated all of the IGM to temperatures above the CMB. The 21-cm signal becomes insensitive to the spin temperature. Emission in 21-cm is now at its strongest before reionization begins in earnest. The 21-cm power spectrum is driven by the fluctuations in the density field. In our fiducial model, this epoch corresponds to $16 \lesssim z \lesssim 18$.

(viii) **Reionization**: Ionizing photons from early generations of sources begin permeating the Universe, wiping-out the 21-cm signal inside ionized regions. The power spectrum initially drops on large scales at $\bar{x}_{\rm HI} \gtrsim 0.9$ as the first regions to be ionized are the small-scale overdensities (McQuinn et al. 2007). The mean signal decreases as HII regions grow, and the power spectrum is governed by HII morphology. This epoch can have other interesting features depending on the detailed evolution of the sources and sinks of ionizing photons, as well as feedback processes, but as the focus of this section is the pre-reionization regime, we shall be brief in this point. In our fiducial model, this epoch corresponds to $7 \lesssim z \lesssim 16$.

---

[25] Note that we discuss global trends here. Locally around each Lyα source, there are partially ionized regions hosting hotter gas (e.g. Cen 2006).